sciendo

Green Sciences, 27, 2, 41—45, 10.2478/pjct-2025-0011

Study on photocatalytic degradation and antibacterial properties of TiO_2/CS composite

Peng Hu, Xiangxiang Wang, Cheng Xu, Mengxi Zhao, Qijie Xu*

College of Chemistry and Pharmaceutical Engineering, Huanghuai University, Zhumadian 463000, P. R. China
**Corresponding author:* e-mail: qijie001@163.com

Capparis spinosa (CS) was extracted by the soxhlet extraction method using ethanol as the extractant. The TiO_2/CS composite was synthesized by the in situ solvothermal method with CS extract as a dopant. The morphology, crystal structure, and optical properties of TiO_2/CS were characterized by SEM, TEM, XRD, UV-Vis and FT-IR spectroscopy. The experimental results showed that TiO_2/CS exhibited excellent photoresponse performance, generated active free radicals, and achieved photocatalytic degradation of organic pollutants. Furthermore, TiO_2/CS served as antibacterial agents to evaluate their antibacterial properties against Escherichia coli (*E. coli*) at different concentrations. The results showed that TiO_2/CS possessed excellent antibacterial performance and produced a significant antibacterial ring, with antibacterial rate of about 100% after being diluted 100 and 500 times, respectively. The test results indicated that TiO_2/CS has great application potential in the field of antibacterial activity and photocatalytic degradation, owing to its advantages of being natural, environmentally friendly, and economical.

Keywords: Capparis spinosa, TiO_2, Photocatalytic degradations, Antimicrobial properties.

Received: 18 February 2025; Accepted: 18 March 2025; Available online: 28.07.2025.

INTRODUCTION

Capparis spinosa (CS) has various functions such as clearing heat and detoxifying, diuresis and swelling reduction, and lowering blood pressure owning to the existence of abundant chemical components of alkaloids, flavonoids, lipids, and glycosides in the structure[1]. CS is a traditional antibacterial drug and has good inhibitory effects on various bacteria[2]. Some studies have reported that the water extract of wild watermelons can completely inhibit the growth of two epidermal fungi (Microsporium canis and Trichophyton purpureum)[2–3]. Ethanol and butanol extracts also possess perfect antibacterial effects on gram-positive bacteria, gram-negative bacteria, Candida albicans, and Aspergillus flavus[4–6]. The research results indicate that the CS extracted from wild watermelon has good antibacterial properties. However, the thermal instability and difficulty in long-term preservation of the extract limit its application. Therefore, combining with other materials to enhance its stability will be a feasible strategy

TiO_2 is equipped with special optical characteristics that can be applied in photocatalytic oxidation, catalytic degradation, photoelectric conversion, etc.[7–8].Especially, TiO_2 has achieved a breakthrough in antibacterial performance through producing reactive oxygen species (ROS). Nevertheless, only the utilization of ultraviolet light in the illumination process and short carrier lifetime impedes their practical applications[9]. Researchers have tried to enhance the antibacterial efficiency by changing the structure of TiO_2. The modification methods mainly include light regulation, doping with metal/non-metallic ions, noble metal modification, and coupling with other materials, and so on[10–13].

CS with the functional groups (-OH, -COO-) can interact with the hydroxyl groups on the surface of TiO_2 to form a stable structure. Furthermore, CS can also provide ROS for TiO_2 to improve its photo-response performance. Therefore, this study aimed to fabricate TiO_2/CS composite by the hydrothermal method using tetrabutyl titanate (TBT) as the titanium source and CS extract as the auxiliary material. Additionally, the photocatalytic degradation and antibacterial performance of TiO_2 and TiO_2/CS were studied. The action mechanism was explored by electron spin resonance (ESR), temperature programmed reduction (TPR).

EXPERIMENTAL SECTION

Reagents

Tetrabutyl titanate (TBT) was supplied by Shandong Tiancheng Chemicals Co. Ltd., China. CS was obtained from Tongrentang pharmacy of Zhumadian city, China. Fecal coliform test kit was purchased from Zhuzhou Hongrun Testing Technology Co. Ltd., China. Methylene blue was provided by Sinopharm Chemical Reagent Co. Ltd., China. All reagents used in this work were of analytical grade and used as received. The water required for the experiment is double-distilled water.

Instruments

The morphology was characterized by scanning electron microscope (SEM, JSM 5600LV, JEOL Ltd., Japan) and transmission electron microscope (TEM, Titan™ G2 60–300, FEI, USA). The crystal structure was gotten by a D/max 2550V X-ray diffractometer (Rigaku, Japan; Cu K_α radiation, λ = 1.54178 Å). The UV-Vis spectra were obtained via a UV-Vis Spectrophotometer (Varian Cary 100, Varian company, American) in the wavelength range of 200–800 nm. Fourier transform infrared (FT-IR) spectroscopy data were collected by Spectrum 2 (Elmer Platinum, American). Electron SSpin Resonance (ESR) spectra were obtained after irradiation by a JES-FA200 EPR spectrometer (JEOL, 9065.8 MHz, X band, 300 K). In addition, the reduction behaviors of Ti element and metallic ions in TiO_2 and TiO_2/CS were evaluated by monitoring the temperature programmed reduction of H_2 with H_2-TPR (DAS-7000, Hunan Huasi, China).

Preparation of TiO_2 and TiO_2/CS nanocomposite

The extract of CS was obtained by using Soxhlet extraction method under the condition of 78 °C, ethanol as extractant (10 times of CS quality) for 6 h. Further, TiO_2 and TiO_2/CS were fabricated via the solvothermal synthesis method. The specific method is as follows: 2 mL of TBT was added to 20 mL of anhydrous ethanol, magnetically stirred for 30 min, the resulting solution was transferred to a 30 mL solvothermal reactor, and heated in a muffle furnace at 210 °C for 24 h. After the reaction was completed, the sample was washed three times with distilled water and anhydrous ethanol, respectively, and finally dried in an oven at 80 °C for 24 h to obtain TiO_2. TiO_2/CS was prepared in the same manner, and appropriate amounts of CS solution and TBT are simultaneously introduced into the solvothermal reactor. The CS doped in the prepared TiO_2/CS composite material is 15% (weight ratio).

Photocatalytic degradation and antibacterial properties of TiO_2 and TiO_2/CS

A certain amount of photocatalyst was added to 100 mL (0.02 M) methylene blue solution and irradiated for a certain period of time under a 500 W photocatalytic device. The absorbance of supernate after centrifugation was measured with a Ultraviolet-visible (UV-Vis) spectrophotometer to calculate the solution concentration and photocatalytic degradation rate. The calculation formula of photocatalytic degradation rate is as follows:

$$v = \frac{A_0 - A_t}{A_0} \times 100\% = \frac{C_0 - C_t}{C_0} \times 100\%$$

Where v represents the degradation rate, A_0 and A_t denote the absorbance of pollutants before and after illumination, and C_0 and C_t are the corresponding pollutant concentrations.

Colitag type *E. coli* detection reagent and Petrifilm 6406 colony count test piece were selected to determine the antibacterial properties of CS, TiO_2, and TiO_2/CS under certain experimental conditions. The testing process was conducted according to the requirements of GB 15979-2024 "Hygienic Standards for Disposable Sanitary Products" issued by tState Administration for Market Regulation (SAMR).

RESULTS AND DISCUSSION

Materials characterization

The morphologies of TiO_2 and TiO_2/CS were first characterized by SEM and TEM. As depicted in Figure 1a, TiO_2 is composed of irregular block particles, whereas TiO_2/CS is in a loose state and composed of irregular spherical particles (Fig. 1c). TEM image shows that TiO_2 appears in granular form, with an average particle size ranging from 70 to 125 nm (Fig. 1b), while TiO_2/CS exhibits an approximately spherical shape with a significantly increased particle size, averaging between 400 and 500 nm. The main reason may be that the CS structure contains abundant functional groups such as carboxyl and hydroxyl groups, which can interact with the hydroxyl groups on the surface of TiO_2 to form a stable structure, inducing the formation of larger TiO_2 particles. Therefore, as a natural polymer material, CS

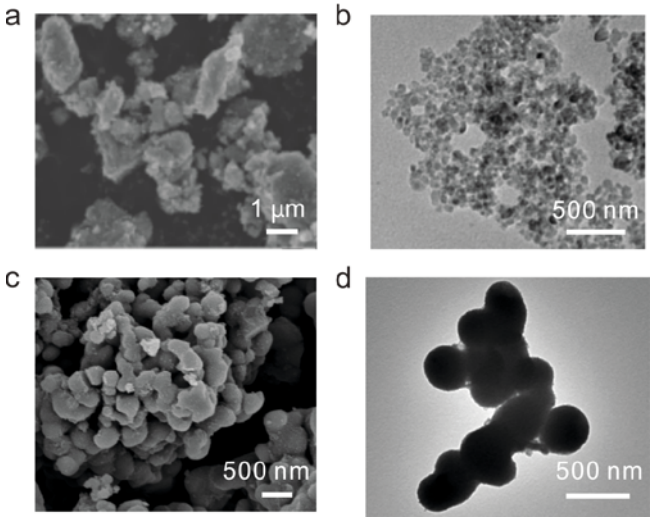

Figure 1. The SEM (a) and TEM images (b) of TiO_2, the SEM (c) and TEM images (d) of TiO_2/CS

is used as a templating agent to induce the formation of TiO_2 nanoparticles and improve the dispersion of the synthesized product[15–16].

The XRD patterns of TiO_2 and TiO_2/CS composite were exhibited in Figure 2a. It can be seen that there are the characteristic peaks of TiO_2 at 27.03^0, 40.92^0, 58.88^0, 60.12^0, 68.5^0, 75.38^0, and 77.08^0,[16] indicating that the introduction of CS did not change the crystal structure of TiO_2. The composite structure and functional group bonding between wild CS and TiO_2 could be analyzed through FT-IR. As shown in Figure 2c, the absorption peaks at 2920 cm^{-1} and 2848 cm^{-1} belong to the stretching vibration absorption peaks of -CH_3 and -CH_2-. The peak of 1720 cm^{-1} is attributed to the stretching vibration absorption of C=O, and the vibrational absorption peaks of -CH_3 appear at 1458 cm^{-1} and 1360 cm^{-1}. The vibrational absorption peak of C-O bond appear at 2092 cm^{-1}, while the absorption peak of C-C belong to 1055 cm^{-1} [17–18]. It can be seen that there are functional groups such as -CH_3, -CH_2-, C=O, and C-O in the infrared spectrum of TiO_2/CS, which is consistent with the external absorption spectrum of CS. The result indicates that a stable structure is formed between TiO_2 and CS, which is due to the bonding effect between CS and TiO_2 functional groups.

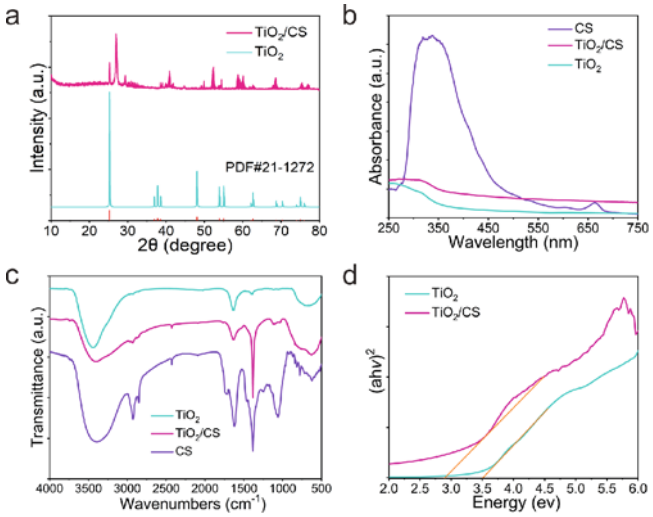

Figure 2. The XRD patterns (a), the UV-Vis spectra (b), the FT-IR spectra (c), and the Tauc Plot (d)

The UV-Vis absorption spectra of CS, TiO_2 and TiO_2/CS were shown in Figure 2b. it could be seen that an absorption peak appears between 200–800 nm, and the peak shapes of TiO_2 and TiO_2/CS are similar, indicating that the addition of CS didn't change the basic structure of TiO_2. The UV-vis data were processed, and the bandgap width of TiO_2 and TiO_2/CS was calculated using the Tauc Plot method. The results were displayed in Figure 2d, the bandgap width of TiO_2 and TiO_2/CS are approximately 3.2 eV and 2.9 eV, respectively, which indicates that the combination of CS and TiO_2 reduces the bandgap width and thus improves the photoactivity[18].

Antibacterial properties of TiO_2, CS and TiO_2/CS

The antibacterial circle experiment can be used to test whether the materials have antibacterial properties. Generally, if the diameter of the antibacterial circle is greater than 7 mm, it indicates that the material has certain antibacterial properties[14, 19]. Taking *E. coli* as the test object, the antibacterial properties of CS, TiO_2, and TiO_2/CS against *E. coli* were investigated, the results were shown in Figure 3a. All three materials have an inhibitory effect on *E. coli*. The diameters of the inhibition zones of CS and TiO_2 are similar, indicating their similar antibacterial performance. The diameter of the antibacterial zone of TiO_2/CS is significantly higher than the previous two, showing better antibacterial performance. The main reason was that the functional groups of the CS structure delayed the recombination of photogenerated electrons and holes in TiO_2, and at the same time, CS has antibacterial activity. The combination of the two materials can better leverage their respective advantages.

Table 1. The comparison of antibacterial rates

Samples	Antibacterial rate/%
TiO_2 (100 times)	85.00 %
TiO_2 (500 times)	80.31 %
CS (100 times)	95.00 %
CS (500 times)	93.00 %
TiO_2/CS(100 times)	≈100.00 %
TiO_2/CS(100 times)	≈100.00 %
Chitosan[20]	95.00%
AgNPs[21]	99.00%

The antibacterial rate is an important indicator for evaluating the antibacterial performance of materials. If the antibacterial rate can reach more than 90%, it can be regarded as an effective antibacterial material. The antibacterial effect of wild CS and its composite materials on *E. coli* was investigated by the plate counting method. As can be seen from Figure 3b, a large number of *E. coli* (more than 80000) grew in the original solution on the plate. After the added antibacterial material was diluted 100 times, no E. coli was found in the CS (Fig. 3c) and TiO_2/CS (Fig. 3e) plates, while only a small amount of *E. coli* (about 50) appeared in the TiO_2 plate (Fig. 3d). The antibacterial rates of the three materials were close to 100%; After 500-fold dilution, 264 *E. coli* were present in the TiO_2 plate (Fig. 3g), while only 38 and less than 10 *E. coli* were observed in the CS (Fig. 3f) and TiO_2/CS (Fig. 3h) plates, respectively. It is evident that the interaction between TiO_2 and CS to form TiO_2/CS does not compromise the antibacterial effect, and the TiO_2/CS can be utilized as an effective antibacterial material. Additionally, the comparison of antibacterial rates of TiO_2, CS, and TiO_2/CS with commercially available products and literature reports is shown in Table 1. It can be seen that the antibacterial rates of TiO_2/CS is better than the reported data[20, 21].

Generally, the abundant functional groups in the CS structure can interact with the hydroxyl groups in the TiO_2, thereby increasing their photoresponse range. This is primarily because the functional groups in CS (such as carbonyl and amino groups, etc.) can not only capture photogenerated holes but also reduce the energy of the valence band and the energy barrier for electron transition. In addition, CS extract can also act as electron capture traps to reduce the recombination probability of photogenerated electrons and holes, thereby improving its catalytic efficiency[24].

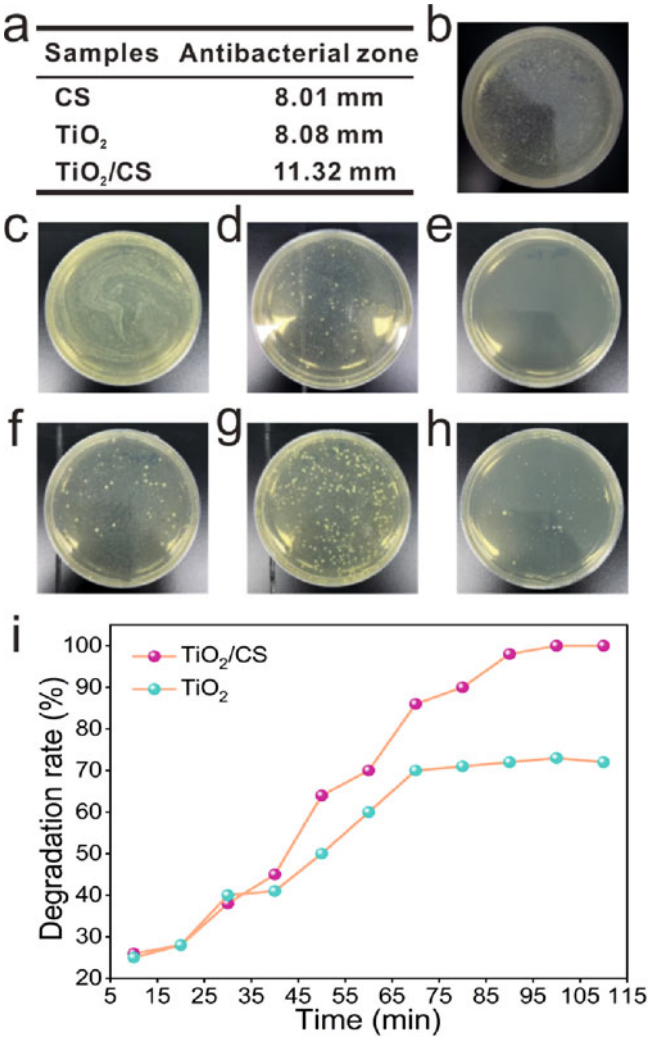

Figure 3. Comparison of the antibacterial regions of the synthesized materials (a), The original solution of *E. coli* (b), the antibacterial activity of CS (c), TiO_2 (d), and TiO_2/CS (e) was diluted 100 times, and the antibacterial of CS (f), TiO_2 (g), and TiO_2/CS (h) was diluted 500 times, (i) The photocatalytic degradation rate of methylene blue by TiO_2 and TiO_2/CS

Photocatalytic degradation properties of TiO_2 and TiO_2/CS

In addition, the photocatalytic degradation rate of TiO_2 and TiO_2/CS was investigated using methylene blue as a simulated pollutant, and the results are shown in Figure 3i. As the illumination time increases, the photocatalytic degradation rate gradually increases after 90 minutes of illumination, and further extension of light irradiation time results in only a marginal increase in the degradation rate. The photocatalytic degradation efficiency of TiO_2/CS for methylene blue reached over 98%, which was significantly better than that of TiO_2. The main reason was that the bandgap width of TiO_2/CS composite material was narrower than that of TiO_2. The addition of CS significantly improved the photoresponse range of TiO_2, and the functional groups in the CS could act as capturing agents to receive photogenerated electrons, thereby reducing the probability of electron-hole recombination, which is beneficial to photocatalytic degradation behavior.

Possible photoactive mechanism

The photocatalytic performance of TiO_2 and its composite materials highly depends on their photoresponse range and adsorption capacity, which is related to the strength of free radicals. By measuring the ESR spectra of photocatalysts, the intensities of superoxide radicals ($\cdot O_2^-$), singlet oxygen ($^1O_2$), and hydroxyl radicals ($\cdot OH$) can be determined, thereby understanding the photocatalytic mechanism of the prepared photocatalyst[19, 22, 23]. The ESR spectra of TiO_2, and TiO_2/CS were presented in Figure 4. The intensity of $\cdot O_2^-$ (Fig. 4a), $\cdot OH$ (Fig. 4b) and $^1O_2$ (Fig. 4c) triggered by TiO_2/CS are higher than that of TiO_2, indicating that doping wild CS in TiO_2 could improve the activity of the photocatalyst, especially its photocatalytic degradation of organic pollutants and inhibition ability against *E. coli*. The main reason was that CS could act as an electron capture agent, promoting the separation of photogenerated electrons and holes in the photocatalytic process, inhibiting their recombination, and prolonging the lifespan of photogenerated electrons and holes.

The activity of various elements in antibacterial materials also affects their photoresponse range and the intensity of free radicals. The temperature-programmed reduction device (TPR) was used to measure the reduction temperature of Ti element in hydrogen atmosphere. The reduction temperature of Ti element in TiO_2 was significantly higher than that of TiO_2/CS, and the TPR curve of TiO_2/CS exhibited certain temperature changes (Fig. 4d). There were two main reasons: (1) functional groups such as carboxyl, amino, and hydroxyl groups in the CS could interact with hydroxyl groups in the surface structure of TiO_2, improving the photocatalytic activity of TiO_2, and generating free radicals. ESR results also proved this; (2) The organic groups contained in the TiO_2/CS underwent chemical changes during the high-temperature hydrogen reduction process, resulting in endothermic phenomena[24–25].

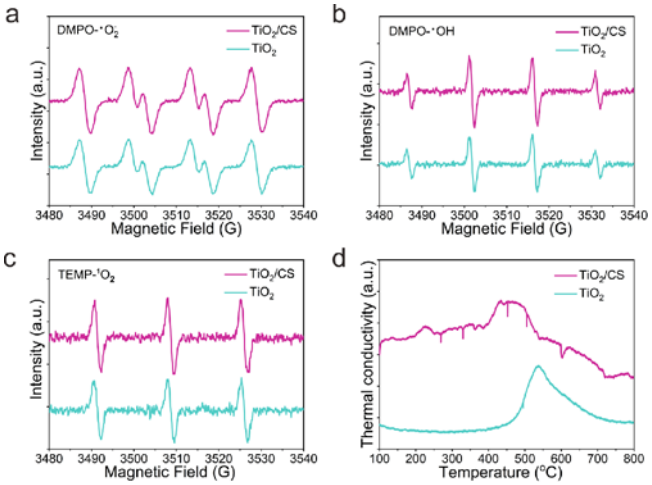

Figure 4. ESR spectra of superoxide free radical (a), hydroxyl radical (b) and singlet oxygen (c), H2-TPR curves (d)

CONCLUSION

CS was obtained by the Soxhlet extraction method using ethanol as the extraction agent. TiO_2/CS was prepared by in situ solvothermal synthesis with CS extract as a dopant. The morphology, crystal structure, and optical properties of TiO_2 and TiO_2/CS were characterized by SEM, TEM, XRD, UV-Vis, and FTIR. The antibacterial performances of CS, TiO_2, and TiO_2/CS were studied by taking *E. coli* as the research object. The results showed that TiO_2/CS had excellent antibacterial performance, even if diluted 500 times, the antibacterial rate could still be achieved at about 100%. Additionally, TiO_2/CS also exhibited perfect photocatalytic degradation of organic pollutants. The results demonstrated that TiO_2/CS had great application potential in antibacterial and photocatalytic degradation.

ACKNOWLEDGEMENTS

This work was supported by the Henan Science & Technology Development Program (Nos. 222102320377, 162102310262 and 172102310660) and Postgraduate Education Reform and Quality Improvement Project of Henan Province (YJS2023JD51)

LITERATURE CITED

1. Sun, Y., Yang, T. & Wang, C. Capparis spinosa L. (2023). Capparis spinosa L. as a potential source of nutrition and its health benefits in foods: A comprehensive review of its phytochemistry, bioactivities, safety, and application. *Food Chem.* 409, 135258. DOI:10.1016/j.foodchem.2022.135258.

2. El-Subeyhi, M., Hamid, L.L. & Gayadh, E.W. (2024). A comprehensive review of its phytochemistry, bioactivities, safety, and application. *Indian J. Microbiol.* 64(2), 548–557. DOI:10.1007/s12088-024-01190-0.

3. Benakashani, F., Allafchian, A.R. & Jalali, S.A.H. (2016). Biosynthesis of silver nanoparticles using capparis spinosa L. leaf extract and their antibacterial activity. *Karbala Int. J. Mod. Sci.* 2(4), 251–258. DOI:10.1016/j.kijoms.2016.08.004.

4. Mansou,r R.B., Jilani, I.B.H. & Bouaziz, M. (2016). Phenolic contents and antioxidant activity of ethanolic extract of Capparis spinosa. *Cytotechnology* 68, 135–142. DOI:10.1007/s10616-014-9764-6.

5. Eid, A. M., Hawash, M. & Abualhasan, M. (2023). Exploring the potent anticancer, antimicrobial, and anti-Inflammatory effects of capparis spinosa oil na noemulgel. *Coatings* 13(8), 1441. DOI:10.3390/coatings13081441.

6. Neamah, S.A., Falih, I.Q. & Albukhaty, S. (2024). Phytochemical characteristic analysis and biological activity for

capparis spinosa L. fruit extract. *Rafidain J. Sci.* 33(1), 68–77. DOI:10.1021/acsomega.3c08314.

7. Xu, Q. & Liu, Z. (2023). Studies on photocatalytic degradation for organic pollutants by TiO_2/Au composite and its antibacterial properties. *Theor. Found. Chem. Eng.* 57(6), 1610-1617. DOI: 10.1134/S0040579523330114.

8. Tang, X., Abdiryim, T. & Jamal, R. (2024). Pyro-phototronic effect enhanced the performance of TiO_2 NRs/BiOCl//PEDOS heterojunction for a UV photodetector. *Chem. Eng. J.* 488, 150940. DOI: 10.1016/j.cej.2024.150940.

9. Aslam, M., Abdullah, A.Z. & Rafatullah M. (2022). Abelmoschus esculentus (Okra) seed extract for stabilization of the biosynthesized TiO_2 photocatalyst used for degradation of stable organic substance in water. *Environ. Sci. Pollut.* 29(27), 41053–41064. DOI: 10.1007/s11356-021-18066-1.

10. Low, J., Zhang, L. & Tong, T. (2018). TiO_2/MXene Ti_3C_2 composite with excellent photocatalytic CO_2 reduction activity. *J. Catal.* 361, 255–266. DOI: 10.1016/j.jcat.2018.03.009.

11. Li, J., Liu, X. & Zhao, G. (2023). Piezoelectric materials and techniques for environmental pollution remediation. *Sci. Total Environ.* 869, 161767. DOI:10.1016/j.scitotenv.2023.161767.

12. Wu M., Zhang M. & Shen L. (2023). High propensity of membrane fouling and the underlying mechanisms in a membrane bioreactor during occurrence of sludge bulking. *Water Res.* 229, 119456. DOI: 10.1016/j.watres.2022.119456.

13. Wu, Q., Huang, J.Y. & Cao, R. (2022). Thermo-, electro-, and photocatalytic CO_2 conversion to value-added products over porous metal/covalent organic frameworks. *Acc. Chem. Res.* 55 (20), 2978–2997. DOI: 10.1021/acs.accounts.2c00326.

14. GB 18466-2005. Discharge standard of water pollutants for medical organization. Beijing China, *China Environmental Science Press*, 2005.

15. Sawal, M.H., Jalil, A.A. & Khusnun, N.F. (2023). A review of recent modification strategies of TiO_2-based photoanodes for efficient photoelectrochemical water splitting performance. *Electrochim. Acta* 143142. DOI: 10.1016/j.electacta.2023.143142.

16. Sandhu, S., Kaur, M. & Sharma, N. (2022). Tailoring the exposed facets of anatase titania and probing their correlation with photocatalytic activity-an experimental and statistical study. *Catal. Sci. Technol.* 12, 6717. DOI:10.1039/D2CY00788F.

17. Zhang, Y., Lei, L. & Plank, J. (2023). Boosting the performance of low-carbon alkali activated slag with APEG PCEs: a comparison with ordinary Portland cement. *J. Sustain. Cem.* 12(11), 1347-1359. DOI:10.1080/21650373.2023.2219253.

18. Govindappa, M., Vishaka, A. & Akshatha, B.S. (2023). An endophytic fungus, Penicillium simplicissimum conjugated with C60 fullerene for its potential antimitotic, anti-inflammatory, anticancer and photodegradation activities. *Environ. Technol.* 44(6), 817–831. DOI: 10.1080/09593330.2021.1985621.

19. Tahir, N., Zahid, M. & Jillani, A. (2023). Impact of alternate Mn doping in ternary nanocomposites on their structural, optical and antimicrobial properties: comparative analysis of photocatalytic degradation and antibacterial activity. *J. Environ. Manage.* 337, 117706. DOI: 10.1016/j.jenvman.2023.117706.

20. Wang, L., Xin, M., Li, M., Liu, W. & Mao, Y. (2023). Effect of the structure of chitosan quaternary phosphonium salt and chitosan quaternary ammonium salt on the antibacterial and antibiofilm activity. *Int. J. Biol. Macromol.*, 242, 124877. DOI: 10.1016/j.ijbiomac.2023.124877.

21. Vadakkan, K., Rumjit, N.P., Ngangbam, A.K., Vijayanand, S. & Nedumpillil, N.K. (2024). Novel advancements in the sustainable green synthesis approach of silver nanoparticles (AgNPs) for antibacterial therapeutic applications. *Coord. Chem. Rev.*, 499, 215528. DOI: 10.1016/j.ccr.2023.215528.

22. Xu, Q., Wang, Y. & Chi, M. (2020) Porous polymer-titanium dioxide/copper composite with improved photocatalytic activity toward degradation of organic pollutants in wastewater: fabrication and characterization as well as photocatalytic activity evaluation. *Catalysts* 10(3), 310. DOI: 10.3390/catal10030310.

23. Liu, Z., Yin, H. & Liu, H. (2024). Antibacterial and photocatalytic degradation properties of TiO_2-based composite. *Anal. Chem.* 104(14), 3295–3302. DOI: 10.1080/03067319.2022.2081080.

24. Sabir, A., Sherazi, T. A. & Xu, Q. (2021). Porous polymer supported Ag-TiO_2 as green photocatalyst for degradation of methyl orange. *Surf. Interfaces* 26, 101318. DOI: 10.1016/j.surfin.2021.101318.

25. Abuzeyad, O.H., El-Khawaga, A.M. & Tantawy, H. (2023). An evaluation of the improved catalytic performance of rGO/GO-hybrid-nanomaterials in photocatalytic degradation and antibacterial activity processes for wastewater treatment: A review. *J. Mol. Struct.* 1288, 135787. DOI: 10.1016/j.molstruc.2023.135787.